Notable Events

The Canterbury, New Zealand Earthquake Sequence II: The Mw 6.2 Christchurch Earthquake of 21 February 2011 and Continuing Aftershock Sequence

John Ristau

GNS Science, Lower Hutt

New Zealand

Excerpt from the
Summary of the Bulletin of the International Seismological Centre:

Ristau, J., The Canterbury, New Zealand Earthquake Sequence II: The Mw 6.2 Christchurch Earthquake of 21 February 2011 and Continuing Aftershock Sequence, *Summ. Bull. Internatl. Seismol. Cent.*, January - June 2011, *48*(1–6), pp. 75–99, Thatcham, United Kingdom, 2015, doi:10.5281/zenodo.998783.

8

Notable Events

8.1 The Canterbury, New Zealand Earthquake Sequence II: The M_W 6.2 Christchurch Earthquake of 21 February 2011 and Continuing Aftershock Sequence

John Ristau
GNS Science
Lower Hutt
New Zealand

8.1.1 Introduction

The moment magnitude (M_W) 6.2 Christchurch earthquake of 21 February 2011 UTC (22 February 2011 NZST) was an aftershock to the 3 September 2010 UTC M_W 7.1 Darfield earthquake that occurred 40 km west of Christchurch (Figure 8.1) (Kaiser *et al.* 2012). Although much smaller than the Darfield earthquake, the Christchurch earthquake was far more devastating to the city of Christchurch, New Zealand's second largest city (population *c.* 377 000). The Christchurch earthquake occurred at shallow depth, ∽6 km SE of the city centre beneath the outer suburbs of Christchurch. The impact of the earthquake was severe, most notably 185 fatalities. The Darfield earthquake occurred at 04:35 on a Saturday morning (NZST) when streets were largely deserted. In contrast, the Christchurch earthquake struck at 12:51 NZST on a weekday when the city centre was highly populated. Building damage, including collapse of some office buildings and widespread damage to heritage structures, was severe. Liquefaction was widespread, and numerous rockfalls and slope failures caused further damage. This was the deadliest earthquake to occur in New Zealand since the 3 February 1931 Hawkes Bay earthquake (M_W 7.4 – 7.6).

The Christchurch earthquake was well recorded (Figure 8.1) by the national GeoNet broadband and strong-motion networks (Petersen *et al.* 2011) and the regional Canterbury CanNet strong-motion network (Avery *et al.* 2004). In addition, more than 180 low-cost micro-electro-mechanical accelerometers were deployed alongside a network of volunteer-owned, internet-connected computers as part of the Quake-Catcher Network (QCN) (Lawrence *et al.* 2014; Cochran *et al.* 2011; Cochran *et al.* 2009). Many of the temporary seismometers and accelerometers installed by GNS Science to record Darfield aftershocks were still operating when the Christchurch event occurred, supplementing the CanNet instruments that provided some of the best near-field ground-shaking measurements.

New Zealand straddles the boundary of the Pacific and Australian plates, and the Canterbury region, where the Darfield and Christchurch earthquakes occurred, is a region of continental convergence across

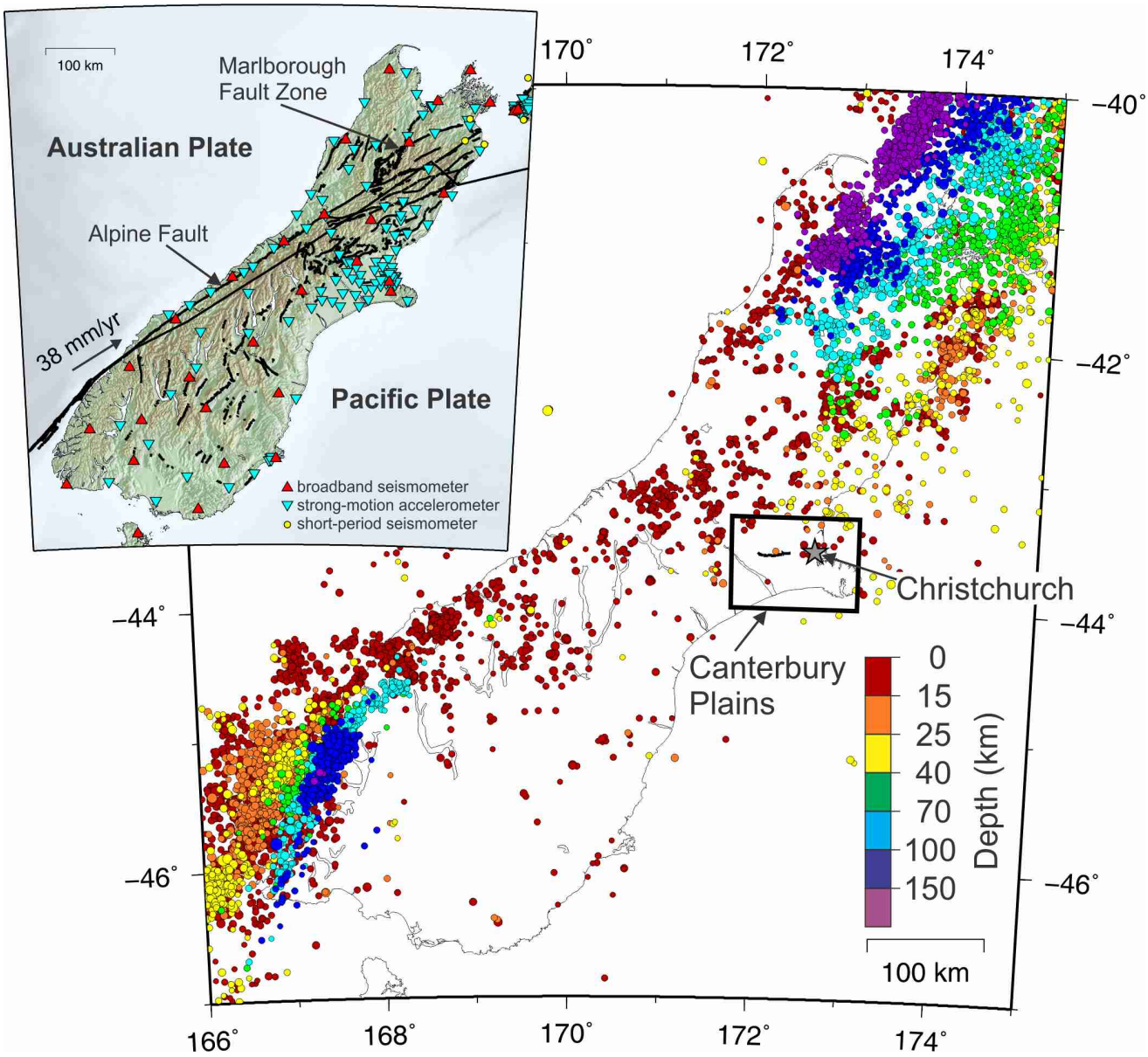

Figure 8.1: *Tectonic setting of the South Island of New Zealand, and recorded seismicity ($M \geq 3$) for the 10-year period until 2 September 2010. Major active faults, including the Alpine Fault and Marlborough Fault Zone, are shown by the black lines. Also shown is the seismograph network of broadband seismometers, strong-motion accelerometers, and short-period seismometers operated by GeoNet. Note the low rate of seismicity in the Canterbury Plains region before September 2010.*

the Pacific/Australia plate boundary (Figure 8.1). In the South Island, the Alpine Fault runs along the west coast and accommodates the vast majority of the relative plate motion. Palaeoseismic evidence suggests that the Alpine Fault ruptures in major earthquakes ($M > 7.5$) with recurrence intervals of $\backsim$200 – 300 years, with the most recent event in 1717 (e.g. Cooper and Norris 1990; Yetton *et al.* 1998; Rhoades and Van Dissen 2003; Sutherland *et al.* 2007; Berryman *et al.* 2012). Several $M > 6$ - 7 earthquakes have occurred in the foothills of the Southern Alps east of the Alpine Fault and west of Christchurch in the past 150 years. These include 1888 North Canterbury M_W 7.1 (Cowan 1991), 1929 Arthur's Pass M_W 7.0 (Doser *et al.* 1999), 1994 Arthur's Pass M_W 6.7 (Abercrombie *et al.* 2000) and 1995 Cass M_W 6.2 (Gledhill *et al.* 2000). The Darfield earthquake demonstrated that the zone of active deformation in the eastern South Island extends beyond the visible range front. There are many mapped active faults in the eastern foothills of the Southern Alps (e.g. Stirling *et al.* 2008); however, no active faults had been previously mapped in the Canterbury plains, including the Christchurch region. Dorn *et al.* (2010) carried out high-resolution reflection seismic studies in the western part of the Canterbury Plains. Unfortunately none of the seismic lines crossed the Greendale Fault.

In this paper I present an overview of the Christchurch earthquake and the continuing aftershock sequence since 21 February 2011. I will discuss the source properties of the Christchurch earthquake, characteristics of the aftershock sequence, and the effect of the earthquake on the city of Christchurch.

8.1.2 The M_W 6.2 Christchurch Earthquake

Before the M_W 7.1 Darfield earthquake the Canterbury Plains region had a historically low level of seismic activity compared with many other parts of New Zealand (e.g. Anderson and Webb, 1994) (Figure 8.1). Typically the largest aftershock in a sequence is about one magnitude unit smaller than the mainshock. For the M_W 7.1 Darfield earthquake the largest aftershock expected was $\backsim M_W$ 6.0, but the largest aftershock was only of M_W 5.0 during the first $5\frac{1}{2}$ months. On 22 February 2011 at 12:51 NZST the M_W 6.2 Christchurch earthquake struck $\backsim$6 km SE of the city centre as an aftershock to the Darfield earthquake.

The Christchurch earthquake occurred on a previously unmapped NE-SW striking fault in the Port Hills area of the outer suburbs of Christchurch (Figure 8.2 a), where there were temporary instruments already installed (Figure 8.2 b). Figure 8.2 c and Table 8.1 show the focal mechanisms from the USGS centroid moment tensor solution (http://earthquake.usgs.gov/regional/neic/), the Global CMT Project solution (http://www.globalcmt.org/) and the GeoNet regional moment tensor solution, all indicating primarily reverse faulting with a strike-slip component. The Christchurch earthquake was far more devastating to Christchurch than the Darfield earthquake due to several factors that will be discussed later, and triggered an extensive aftershock sequence centred around Christchurch and into Pegasus Bay east of Christchurch, mostly notably a M_W 6.0 aftershock on 13 June 2011 UTC.

In the $5\frac{1}{2}$ months following the M_W 7.1 Darfield earthquake much of the aftershock activity had been focused in the Canterbury Plains west of Christchurch. Aftershock activity also extended east of the Greendale Fault towards Christchurch, most notably the 26 December 2010 NZST (25 December 2010 UTC) cluster of aftershocks that occurred near the city centre (Ristau 2011). The Christchurch earthquake occurred east of the main aftershock zone in an area of small positive stress resulting from the

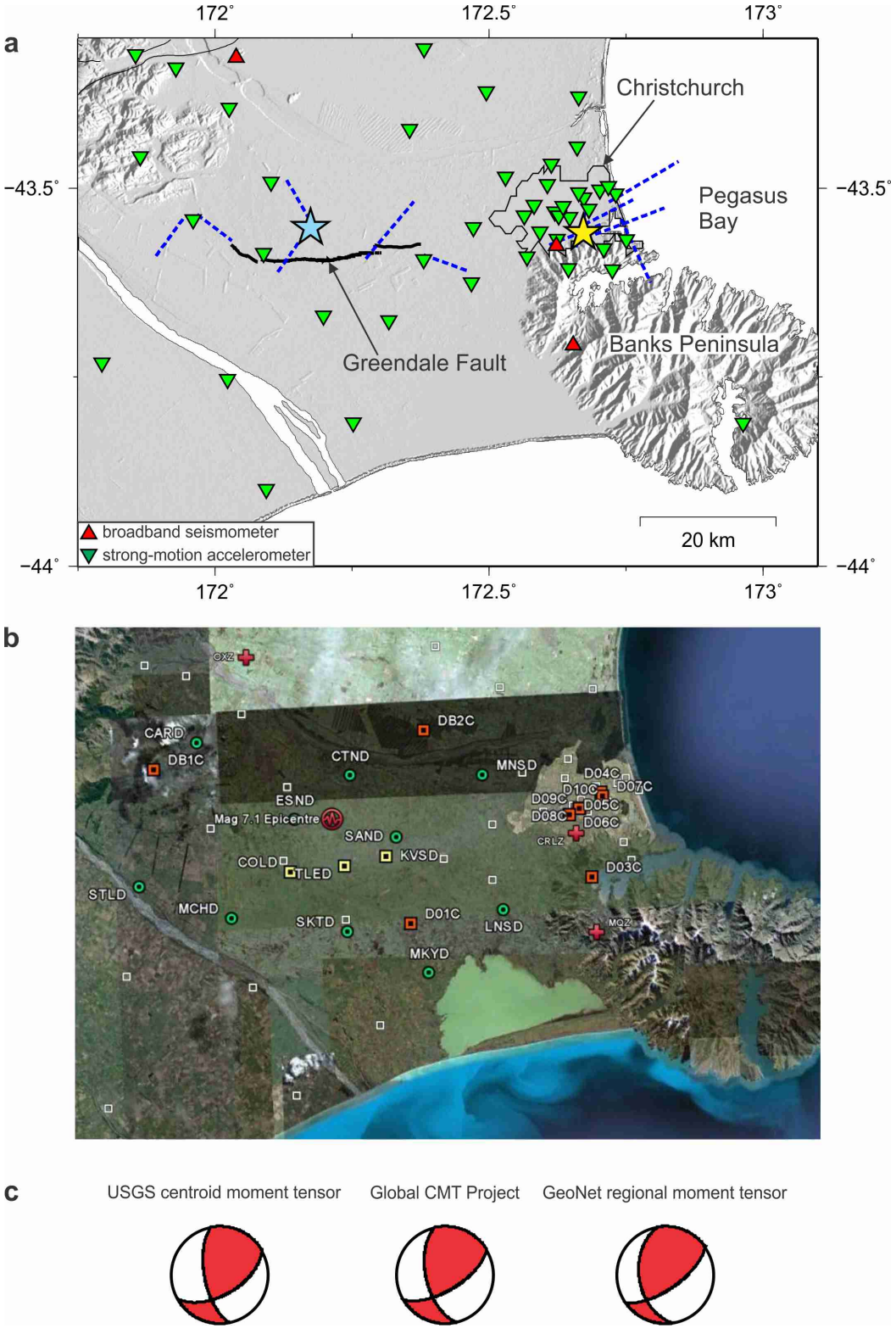

Figure 8.2: *(a) Seismograph network in the Canterbury region at the time of the M_W 7.1 Darfield earthquake (blue star). The yellow star is the location of the M_W 6.2 Christchurch earthquake. Inferred subsurface faults (dashed lines) are those of Beavan et al. (2012), Elliot et al. (2012) and Atzori et al. (2012). Broadband seismometers are indicated by red triangles and regional Canterbury CanNet strong-motion accelerometers by inverted green triangles. (b) Temporary short-period seismometer (green circles), accelerometer (yellow and orange squares) network installed immediately following the Darfield earthquake, along with CanNet strong-motion accelerometers (white squares). (c) Focal mechanisms for the Christchurch earthquake from the USGS centroid moment tensor solution, the Global CMT Project solution and the GeoNet regional moment tensor solution.*

Table 8.1: *Source parameters for the February 2011 Christchurch earthquake.*

Agency/Type	strike/dip/rake	strike/dip/rake	Mo (Nm)	M_w	Depth (km)
USGS centroid moment tensor	59/59/147	168/62/36	1.86E+18	6.1	12
Global CMT Project	59/64/143	167/57/32	1.92E+18	6.1	12
GeoNet regional moment tensor	55/66/129	172/44/35	2.46E+18	6.2	4

Darfield earthquake (Kaiser *et al.* 2012).

One of the most notable features of the Christchurch earthquake were the high peak ground accelerations (PGA's), observed up to 2.2 g vertically and 1.7 g horizontally at Heathcote Valley ∽2 km from the epicentre. In the city centre vertical PGA's of 0.8 g and horizontal PGA's of 0.7 g (Figure 8.3) were recorded (Kaiser *et al.* 2012). The deep Christchurch sedimentary basin likely led to a waveguide effect for the seismic waves, which resulted in increased ground motion durations and long-period amplitudes (Bradley and Cubrinovski 2011; Bradley 2013). These PGA's are among the highest recorded worldwide; a similar analogue globally is the 2008 M_W 7.2 Iwate-Miyagi, Japan earthquake with PGA > 3.9 g (Suzuki *et al.* 2010).

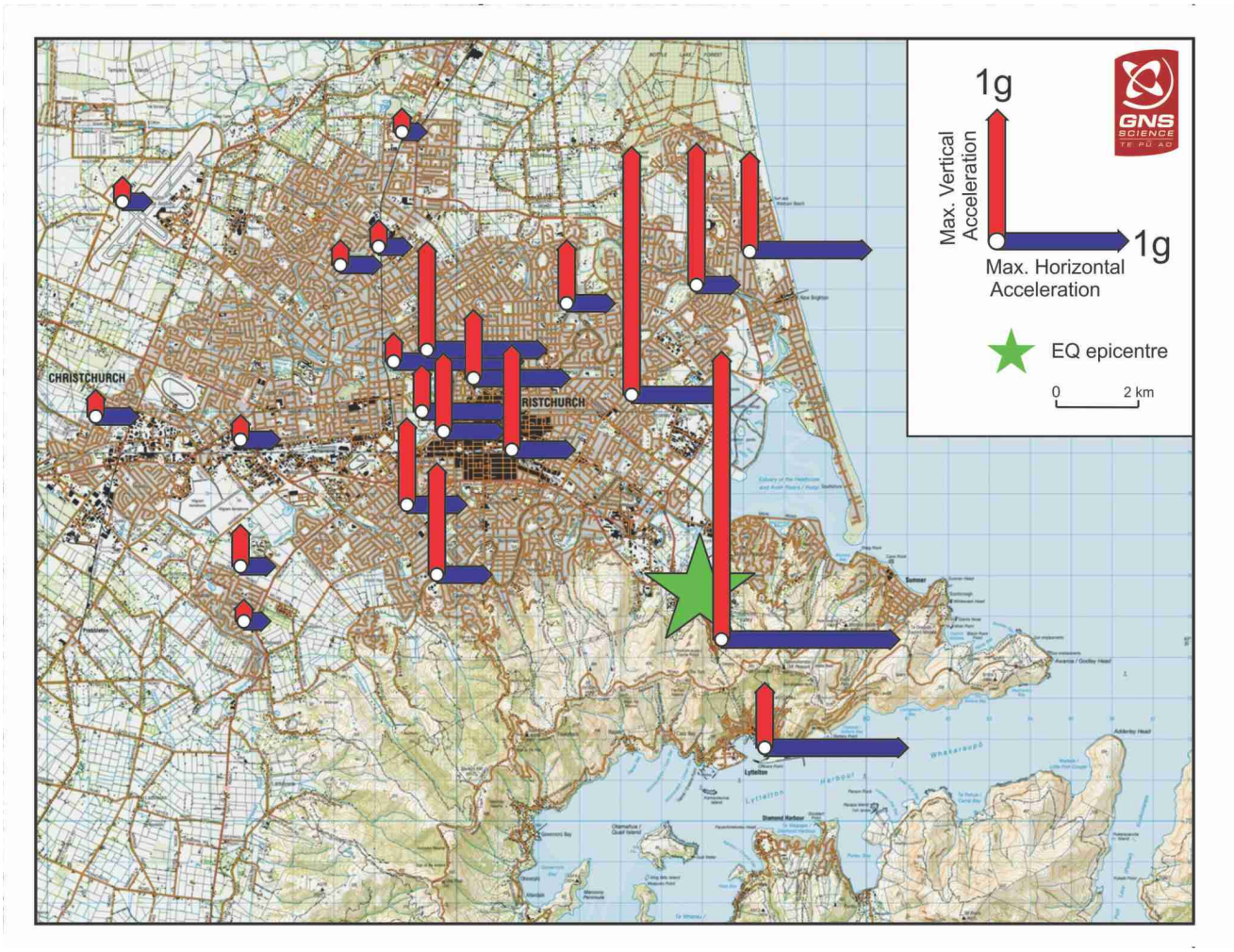

Figure 8.3: *Map of the Christchurch urban area showing maximum PGA (vertical and horizontal components).*

A kinematic source model for the Christchurch earthquake with a rupture velocity of 2.8 km/s and a maximum slip of 4.2 m (Figure 8.4) was calculated using data from 11 strong-motion stations within 20 km of the epicentre (Holden 2011). The slip model, in which the maximum slip is located at ∽4 km depth and occurred north and up-dip of the hypocentre, shows the S-wave energy being directed up-dip towards Christchurch. A high rupture velocity is also noted in Fry *et al.* (2011); based on data filtered up to 5 Hz, they require a rupture velocity of 3.2 km/s to reproduce the high accelerations near the source. The waveform data used for the kinematic source model shows a dominant peak in the velocity records a few seconds after the main rupture. For stations in central Christchurch this signal is larger than the signal modelled from the initial slip and suggests more than one subevent may have been involved in the rupture. A similar result was found in the kinematic model of Serra *et al.* (2013). Fry and Gerstenberger (2011) calculated radiated energy (ES) estimates from broadband P-waves that gave an energy magnitude of Me 6.8 for the Christchurch earthquake. Apparent stress, defined as the product of rigidity and ES per unit moment, was calculated by Fry and Gerstenberger (2011) to be ∽4.1 MPa, higher than global averages (e.g. Choy *et al.* 2001; Atkinson and Boore 2006).

As with the Darfield earthquake, geodetic studies of the Christchurch earthquake involving GPS and InSAR data have been carried out by Beavan *et al.* (2012), Elliot *et al.* (2012) and Atzori *et al.* (2012). All of the geodetic models require multiple fault segments to be active during the rupture. Beavan *et al.* (2011) presented single-fault and two-fault models of the rupture, but acknowledged that a region of apparent ground uplift in eastern Christchurch was not fit by their models. Beavan *et al.* (2012) incorporated LiDAR data for the region into their geodetic model, to better constrain the uplift in eastern Christchurch, and proposed a three-fault model (Figure 8.5) with the eastern section having oblique reverse/right-lateral faulting, the western section having mainly right-lateral faulting, and the NNE-trending cross-fault having nearly pure reverse faulting. The moment release is similar for all three segments with a total moment release of M_0 4.07×10^{18} Nm, equivalent to an event with M_W 6.4. The multiple fault segments required by the geodetic models are consistent with the kinematic source model, and the large strike-slip segment required by Beavan *et al.* (2012) agrees with the kinematic results. The two-fault geodetic models proposed by Elliot *et al.* (2012) and Atzori *et al.* (2012) have most of the moment release along a reverse faulting segment, but also require a large strike-slip segment.

The crustal structure in the Canterbury region is dominated by the Hikurangi Plateau – a large igneous province subducted ∽100 million years ago. The Hikurangi Plateau is extremely strong and remains attached to the crust, capped by schist and greywackes containing east-west Cretaceous faults (Reyners *et al.* 2014). Reyners *et al.* (2014) found unusually low P- to S-wave ratios of 1.60, in contrast to velocity ratios of 1.71 before the Darfield earthquake. They interpreted the reduced velocity ratios as a signature that the greywackes had been weakened by the rupture front producing widespread cracking around the fault zone, and suggested that recovery of rock strength between the Darfield and Christchurch earthquakes could explain the long delay between the two events.

As mentioned above, the Christchurch earthquake was far more devastating to the city of Christchurch than the Darfield earthquake, despite being much smaller. The most important factor was the proximity of the Christchurch earthquake to the city compared with Darfield. The Christchurch earthquake occurred beneath the outer suburbs of Christchurch ∽6 km SE of the city centre, whereas the Darfield earthquake occurred ∽40 km west of Christchurch and the eastern end of the rupture zone was ∽20 km

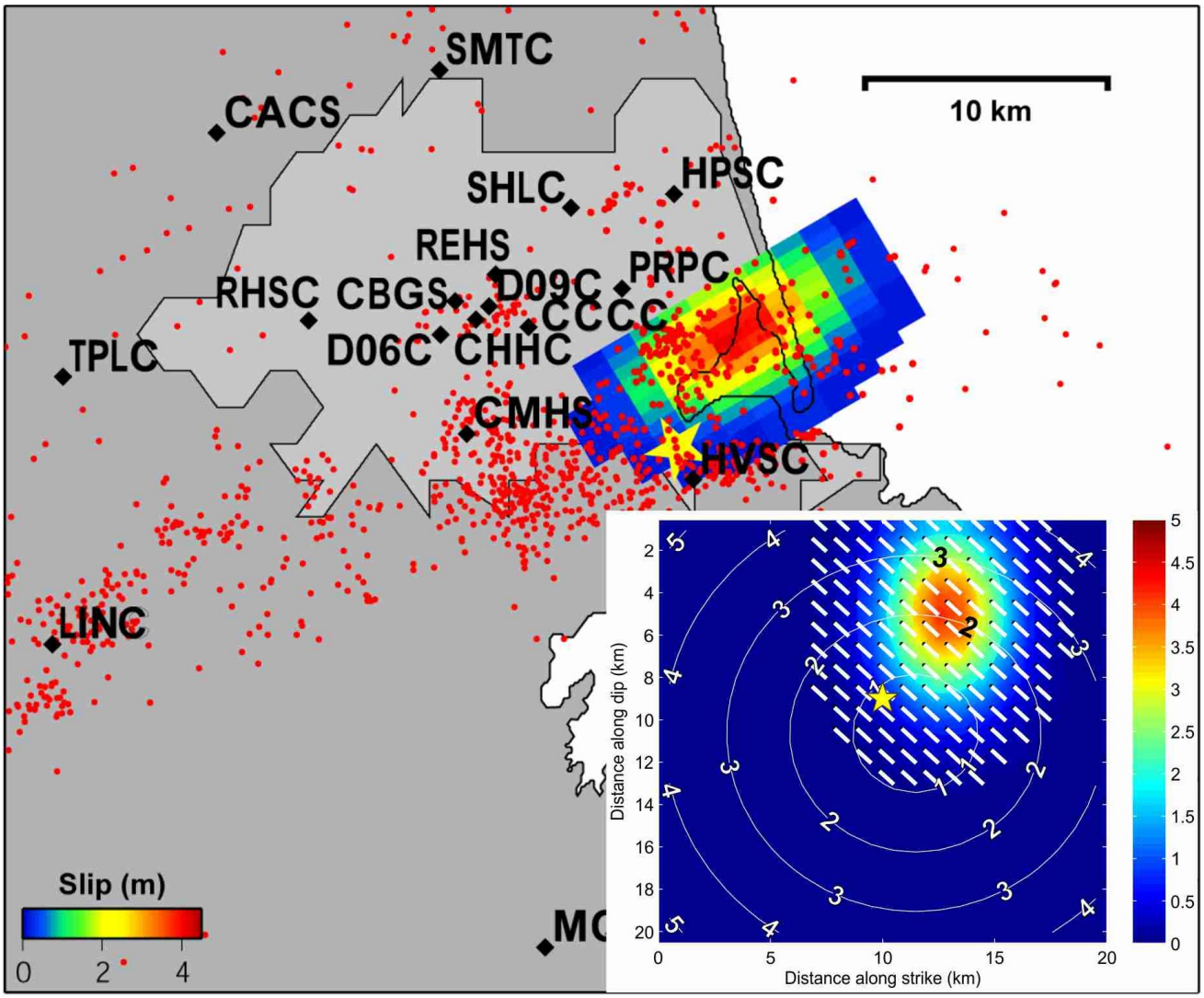

Figure 8.4: *Map view of the slip distribution on a plane with strike 59° and dip 67° SSE. Aftershock locations (red dots) and the Christchurch epicentre (yellow star) are from Bannister et al. (2011), and black diamonds are strong-motion instruments used to calculate the slip distribution. The inset shows the vertical projection of the slip distribution with the slip direction indicated by the white vectors, showing the energy being directed updip towards Christchurch. Rupture front propagation timing in seconds is indicated by the white contours (from Holden, 2011).*

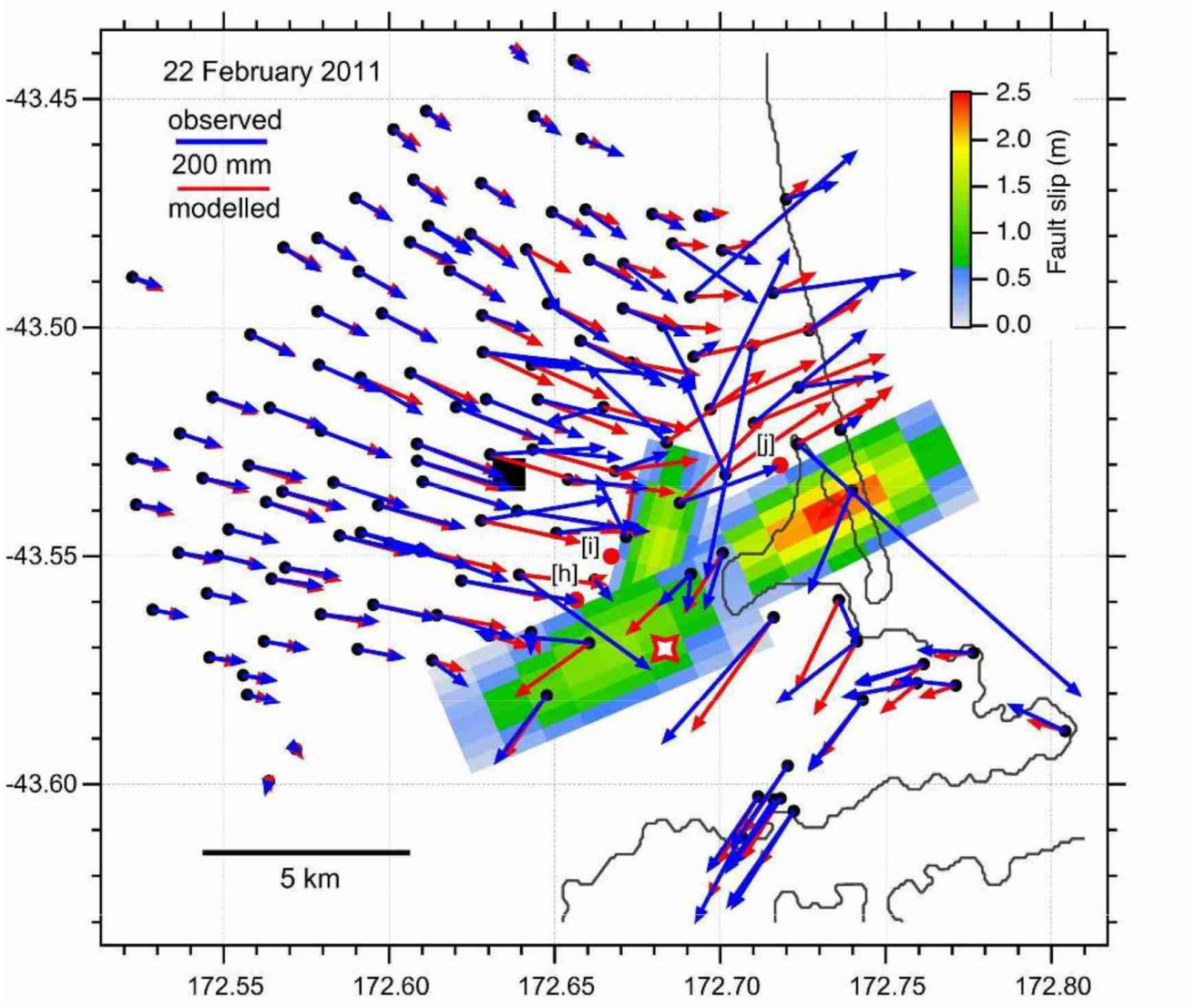

Figure 8.5: *Observed (blue) and modelled (red) displacements at GPS sites and the slip model derived from GPS and DInSAR data for the Christchurch earthquake. Red dots with adjacent letters in square brackets (e.g. [a]) are located where the centres of the fault segments would outcrop if extended to the surface (from Beavan et al. 2012).*

west of Christchurch. Another important factor was the great amount of radiated energy produced and the effects of strong source directivity where much of the energy was directed towards the city (Fry *et al.* 2011; Holden 2011).

A third important factor involved the response of the shallow subsurface to extreme ground motions. Fry *et al.* (2011) found that strong-motion recordings at several near-source sites in the city contained much higher frequency content on the vertical component compared with the corresponding horizontal component. They interpreted this phenomenon as being due to the presence of a shallow water table that dramatically attenuated the propagation of high-frequency shear waves. The vertical components exhibited a high degree of asymmetry (Figure 8.6) with maximum accelerations in the upward direction ($> 1\ g$) exceeding accelerations in the downward direction ($< 1\ g$).

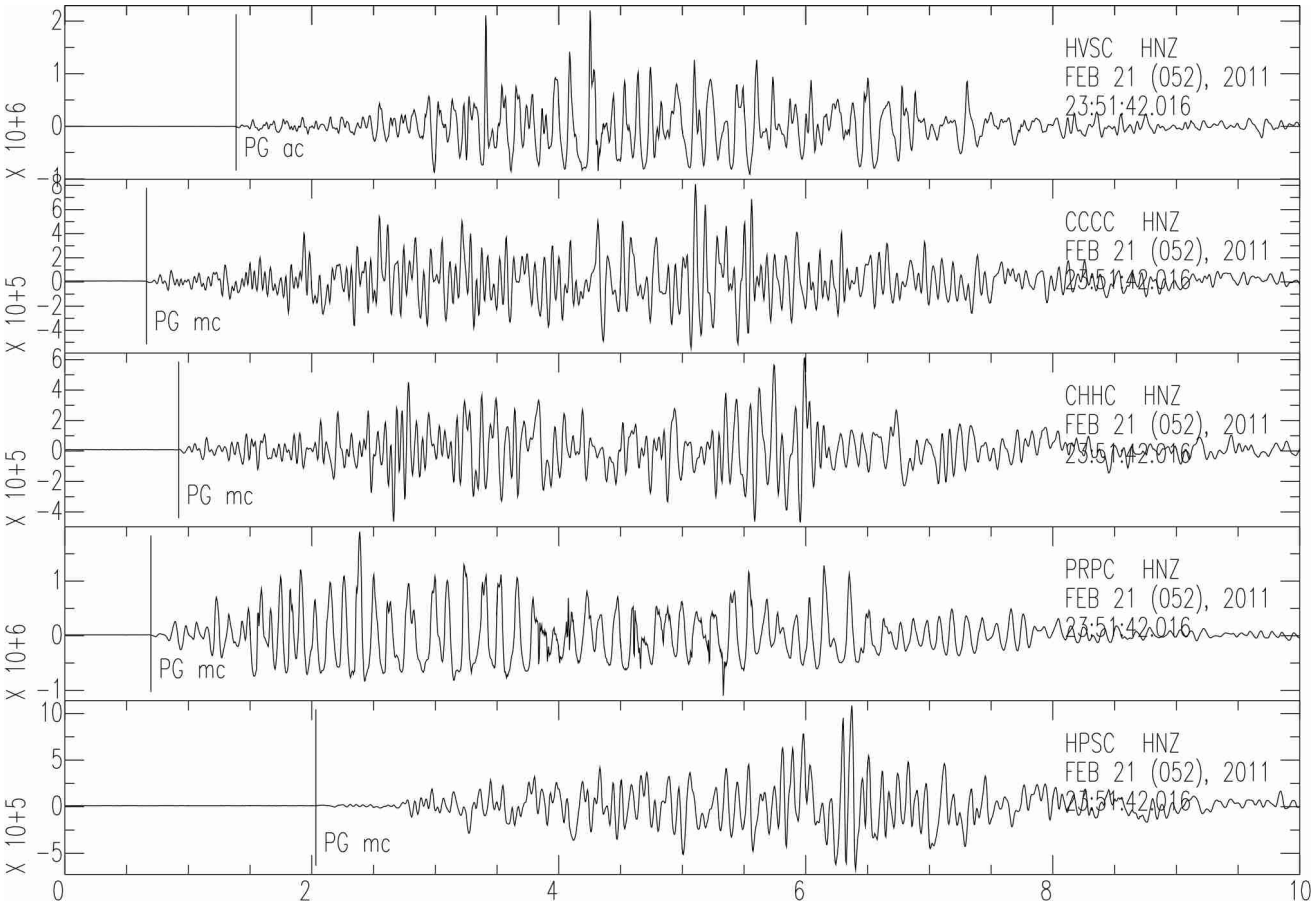

Figure 8.6: *Vertical acceleration waveforms from strong-motion sites in the Christchurch region, showing larger positive accelerations than negative ones. Many of the negative acceleration troughs are also broader than the narrow positive spikes (from Fry et al. 2011).*

Asymmetric vertical recordings were also noted during the 2008 M_W 6.9 Iwate-Miyagi Nairiku, Japan earthquake (Aio *et al.* 2008; Yamada *et al.* 2009) and attributed to a "trampoline" effect. Aoi *et al.* (2008) describe the asymmetry as due to the decoupling of near-surface materials during high-amplitude downward acceleration, resulting in an approximate free-fall of the material. Yamada *et al.* (2009) suggests that the large positive accelerations are further enhanced by "slapdown", as free-falling upper soil layers impact with deeper layers that are returning upwards following the earthquake wave cycle. Fry *et al.* (2011) interpreted the asymmetry in the Christchurch vertical accelerations as being due to the "trampoline" and "slapdown" effects, which further intensified the ground shaking and subsequent

damage.

8.1.3 Effects on the built environment

Liquefaction

One of the significant effects of the Christchurch earthquake was widespread liquefaction throughout the urban areas of the city (Figure 8.7), causing extensive damage to residential properties, water and wastewater networks, high-rise buildings and bridges. Liquefaction was evident from massive sand boils and from large amounts of sand/silt ejecta and water throughout the city. Nearly 15 000 homes were severely damaged, with more than half beyond repair (Cubrinovski *et al.* 2012; Reid *et al.* 2012; Cox *et al.* 2012). The greatest damage occurred along the Avon River, which flows through the city centre, with permanent lateral spreading at the riverbanks of up to 2 – 3 m that progressed as far as 200 – 250 m inland, causing significant damage to structures within the spreading zone (Cubrinovski *et al.* 2012).

Landslides

The large accelerations, combined with the proximity of the earthquake to the Port Hills, triggered numerous landslides in the southern suburbs of Christchurch (e.g. Massey *et al.* 2014). At least five deaths there were attributed to falling rocks. Several hundred homes were evacuated because they were close to the foot or top of dangerous cliffs. Four main types of earthquake-triggered mass movements were identified: rockfalls, shallow landslides, deep-seated landslides and tension cracks (Figure 8.8). Rockfalls made up the majority of the mass movements and caused substantial damage to properties. Some rockfalls travelled large distances to smash through houses and ranged from single boulders to large masses of rock. Many slopes showed deep tension cracks and rents that indicated rock sections with potential for further collapse.

Building damage

The damage to buildings in Christchurch varied considerably depending on the site location, extent of liquefaction at the site and the building characteristics. The building stock in Christchurch consists of unreinforced masonry buildings, timber buildings, reinforced concrete buildings and tilt-up (pre-fabricated) industrial buildings. Damage to masonry buildings including churches (e.g. Figure 8.9; Figure 8.10) was widespread across the city. Residential and commercial unreinforced masonry buildings also performed poorly and suffered significant structural damage (Figure 8.10). Timber homes generally performed better; however, many homes suffered significant damage due to lateral spreading from liquefaction (e.g. Fleischman *et al.* 2014; Sritharan *et al.* 2014). Modern reinforced buildings generally performed well, mostly sustaining only moderate damage. But in the Christchurch city centre, many of the fatalities resulted from the almost complete collapse of the Canterbury Television (CTV) building and the Pyne Gould building. Another example of severe damage was the historic Time Ball Station in Lyttelton, SE of Christchurch.

Figure 8.7: *(a) Liquefaction area behind the Catholic Basilica, Christchurch, photographer Margaret Low, copyright GNS Science, VML ID 6141. (b) Car trapped by liquefaction, photographer Andrew King, copyright GNS Science, VML ID 101933.*

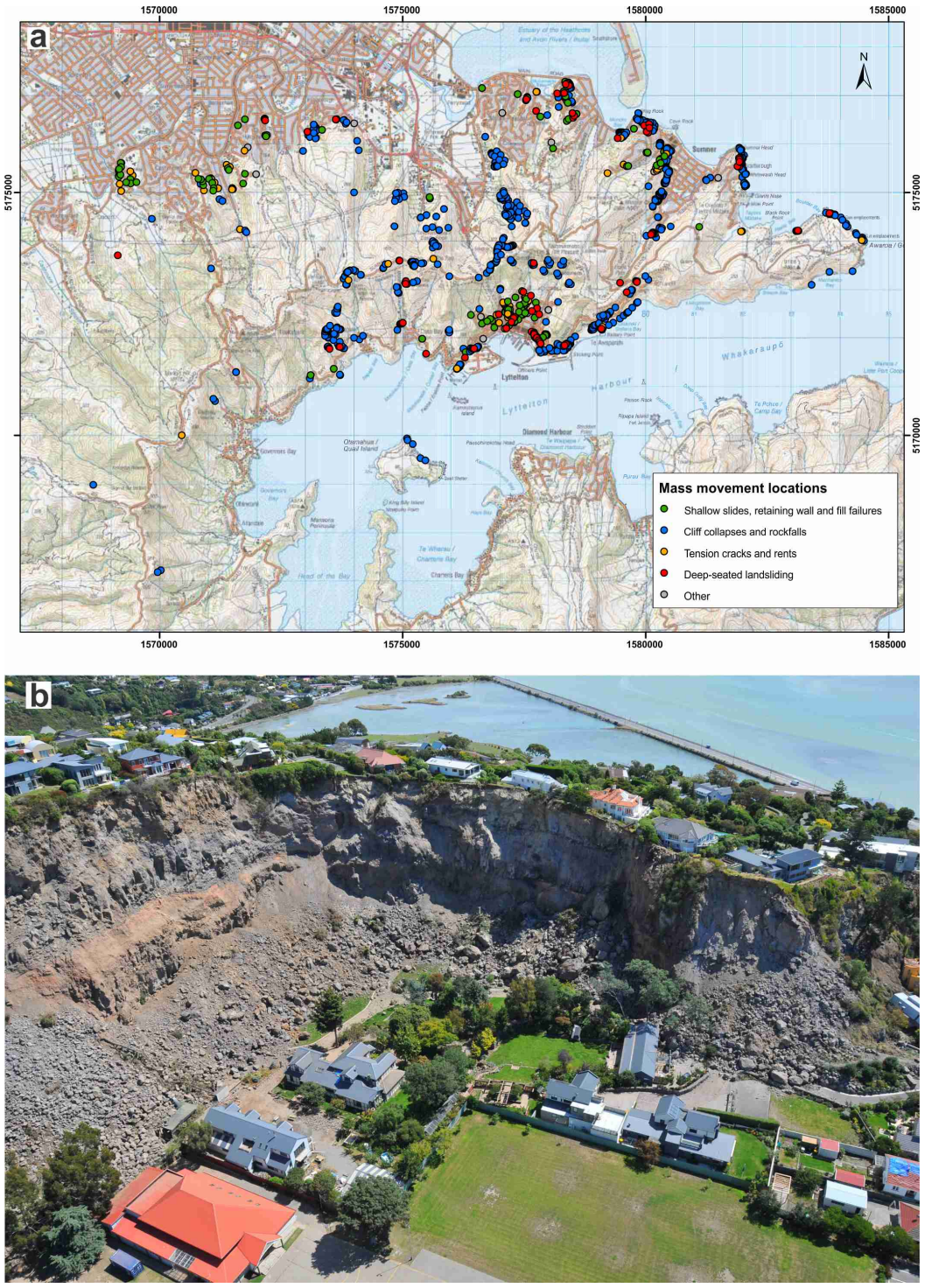

Figure 8.8: *(a) Map showing the distribution of mass movements caused by the Christchurch earthquake (from Massey et al. 2014). (b) Example of earthquake induced mass movement showing the proximity of homes at the top and base of the cliff, photographer Graham Hancox, copyright GNS Science/EQC, VML ID 130503.*

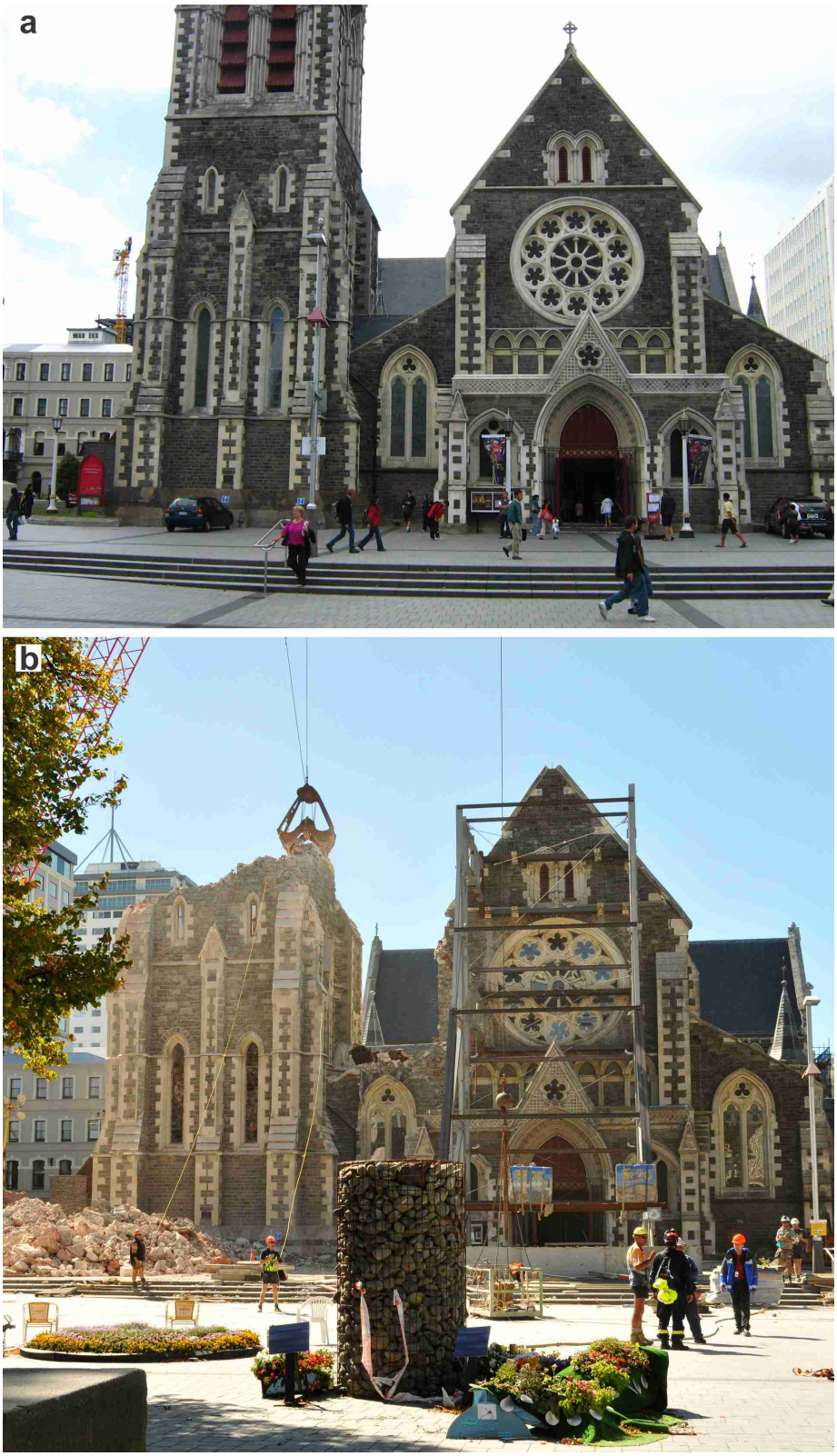

Figure 8.9: *(a) The historic Christchurch Cathedral in the city centre before the Christchurch earthquake. (b) Christchurch Cathedral after the Christchurch earthquake, photographer Margaret Low, copyright GNS Science, VML ID 6175.*

Figure 8.10: *(a) Damage to the Cathedral of the Blessed Sacrament, photographer Margaret Low, copyright GNS Science, VML ID 6128. (b) Damaged building, photographer Margaret Low, copyright GNS Science, VML ID 101912. (c) Building damage in the Christchurch central business district, photographer Margaret Low, copyright GNS Science, VML ID 101881.*

8.1.4 Aftershock Sequence

The M_W 6.2 Christchurch earthquake initiated a rejuvenated aftershock sequence, mainly centred near the city of Christchurch and the Pegasus Bay offshore region (Figure 8.11 a). More than 4400 of the aftershocks, with $M_L \geq 1.0$ and with 13 $M_W \geq 5.0$, were relocated using a double-difference tomography method (Bannister *et al.* 2011). The most significant of these included the M_W 6.0 aftershock of 13 June 2011 UTC, located ∽4 km east of the Christchurch earthquake epicentre, and a later sequence of large M_W 5.4 – 5.9 aftershocks on 23 December 2011 UTC, which occurred in Pegasus Bay, NE of the Christchurch earthquake epicentre. The aftershocks from 21 February – 13 June 2011 occurred mainly in the southern parts of Christchurch with some extension west of the city. A feature of the aftershocks is that they do not clearly define the fault plane of the Christchurch earthquake as defined by either the moment tensor solution or the geodetic model (Bannister *et al.* 2011), suggesting that there may have been very little post-seismic slip on the fault.

The M_W 6.0 earthquake of 13 June 2011 UTC was a strike-slip event that occurred ∽4 km east of the Christchurch earthquake epicentre (Figure 8.11; Sibson *et al.* 2011). The geodetic model from Beavan *et al.* (2012) suggests two possibilities for this event. The first possibility is a single-fault model with the rupture on a NNW-SSE striking plane. The second possibility is a two-fault model with rupture on a NNW-SSE striking plane and on a ENE-WSW striking plane, with approximately equal moment release on each plane. Beavan *et al.* (2012) were unable to distinguish between the two options, but preferred the two-fault model that was mainly consistent with the kinematic source model of Holden and Beavan (2012). The first event on the ENE-WSW plane ruptured a region 6 km × 5 km with a maximum slip of 3 m, and the second event on the NNW-SSE plane ruptured a region 11 km × 7 km with a maximum slip of 2.6 m (Holden and Beavan 2012).

The 13 June 2011 earthquake reinvigorated the sequence with many aftershocks extending SE into Banks Peninsula where little aftershock activity had occurred previously. It caused further damage and liquefaction in Christchurch but its effects were significantly less than for the Christchurch earthquake. Whereas the Christchurch earthquake had mainly reverse faulting, focal mechanisms derived from regional moment tensor solutions for aftershocks to the Christchurch earthquake and this later earthquake indicated mainly strike-slip faulting, though there were some with reverse or oblique-reverse faulting (Figure 8.11 b).

Three earthquakes on 23 December 2011 UTC (M_W 5.4 – 5.9) centred near Pegasus Bay, east of Christchurch, triggered a NE-SW series of aftershocks that extended offshore. These earthquakes were widely felt in Christchurch but damage was minimal due to their offshore location (Ristau *et al.* 2013). The M_W 5.9 event indicated reverse faulting and the kinematic solution favoured a SE-dipping fault plane with a slip region of 18 km × 15 km with a maximum slip of 0.8 m. Due to the offshore location it was not possible to determine a well-constrained geodetic model. Fifty-three focal mechanisms were determined for events in Pegasus Bay with a majority (45 of 53) indicating reverse or oblique-reverse faulting. This is in contrast with the rest of the Canterbury aftershock sequence where ∽74% of the focal mechanism determinations indicated strike-slip faulting (Ristau *et al.* 2013).

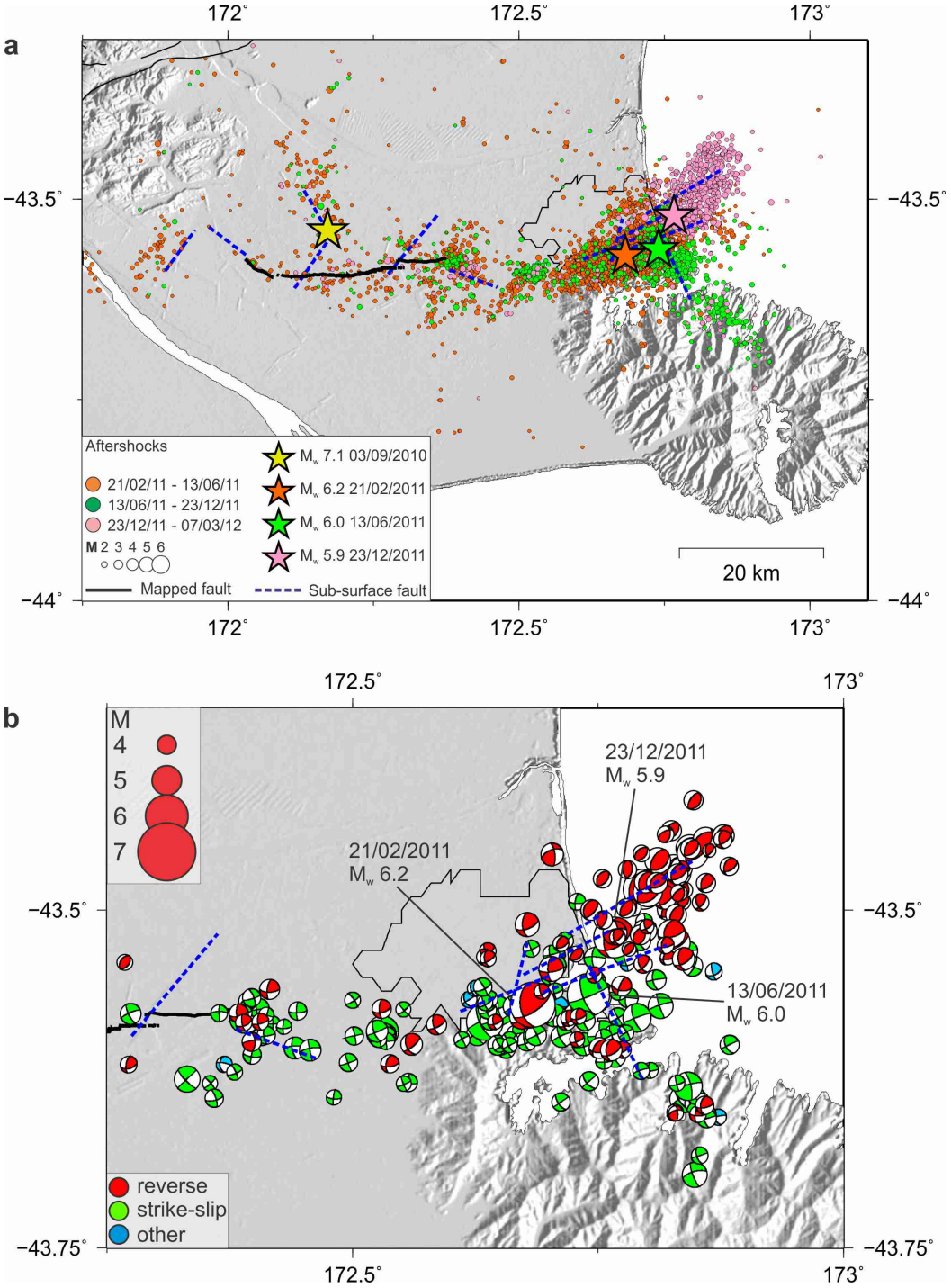

Figure 8.11: *(a) Relocated aftershocks for the period 21 February 2011 – 31 January 2012. The solid black line represents the Greendale Fault and the dashed blue lines the inferred subsurface faults. Stars show the epicentres of the Darfield earthquake, the Christchurch earthquake, and later large aftershocks closer to Pegasus Bay. Aftershocks symbols are colour coded to correspond to each of the main earthquakes and before the next earthquake. Aftershocks preceding the Christchurch earthquake are not shown. (b) Focal mechanisms derived from 204 regional moment tensor solutions for the period 21 February 2011 – 20 November 2013.*

8.1.5 Stress Studies and Aftershock Forecasts

Steacy *et al.* (2014) studied stress triggering during the Canterbury earthquake sequence by comparing maps of Coulomb stress changes with the location of later events. They investigated whether later large aftershocks were consistent with stress triggering, and whether a simple stress map produced shortly after the Darfield earthquake would have accurately indicated the regions where subsequent activity occurred. Steacy *et al.* (2014) found that all aftershocks with $M > 5.5$ occurred in areas of increased failure stress computed using a slip model for Darfield that was available within 10 days of its occurrence. The Christchurch earthquake was in a region of small positive stress induced by the Darfield earthquake (Figure 8.12; C. Williams pers. comm.); however, the Christchurch earthquake was preceded by a M 5 earthquake on 7 September 2010, centred ∽2.3 km away that may have increased the stress locally by 4.2 MPa (Steacy *et al.* 2014). The June 2011 earthquake also occurred in a region of positive stress induced by the Darfield earthquake and was preceded by four $M \geq 5$ events (22 February, 5 March, 16 April, and 13 June 2011) within a few kilometres of its epicentre (Steacy *et al.* 2014). Ristau *et al.* (2013) examined the Coulomb stress changes near Pegasus Bay using the modelled Darfield, Christchurch and June 2011 events as source faults. They found that the epicentral region for the December 2011 Pegasus Bay earthquakes had positive stress regions at very shallow depths (∽6 km), but mainly regions of negative stress at greater depths. The hypocentres for the Pegasus Bay earthquakes were largely at depths greater than ∽5 km with an average depth of ∽10 km.

The aftershock probability forecasts continued to evolve throughout the Canterbury earthquake sequence as each large earthquake reinvigorated the aftershock sequence (e.g. Gerstenberger *et al.* 2014). Table 8.2 shows how the expected number aftershocks in the M 4.0 – 4.9 and $M \geq 5.0$ ranges changed later in the Canterbury aftershock sequence. Immediately after the Christchurch earthquake the expected number of aftershocks with $M \geq 4.0$ had decreased to low levels and it then increased dramatically afterwards. The same pattern occurred immediately before and after the June 2011 earthquake. The aftershock forecasts underestimated the number of aftershocks in the M 4.0 – 4.9 range immediately following each main earthquake, as had been the case also after the Darfield earthquake. Subsequently the observed numbers of aftershocks were mainly in agreement with the forecasts.

Table 8.3 shows one-week, one-month, and one-year aftershock probabilities for M 5.0 – 5.9, M 6.0 – 6.9 and M 7.0+ at three dates after the Christchurch earthquake. These probabilities are valid for the entire Canterbury Plains region, including Christchurch, but were calculated while the catalogue was still being revised and completed (A. Christophersen, pers. comm.). Following the Christchurch earthquake the one-week and one-month probabilities were ∽2 – 3 times above earlier 27 January 2011 forecasts, but the one-year probabilities remained about the same. From 1 November 2013 the one-year probability for a M 5.0 – 5.9 was still high (68%), but low for $M \geq 6.0$, with similar results for 1 April 2014. Thus the aftershock probabilities are diminishing but not negligible. The lesson here has been that the Canterbury sequence has been long-lasting with multiple reinvigoration.

8.1.6 Discussion

In this paper I have summarised some of the major findings of the M_W 6.2 Christchurch earthquake, the subsequent aftershock sequence and its relationship to the M_W 7.1 Darfield earthquake. The Canter-

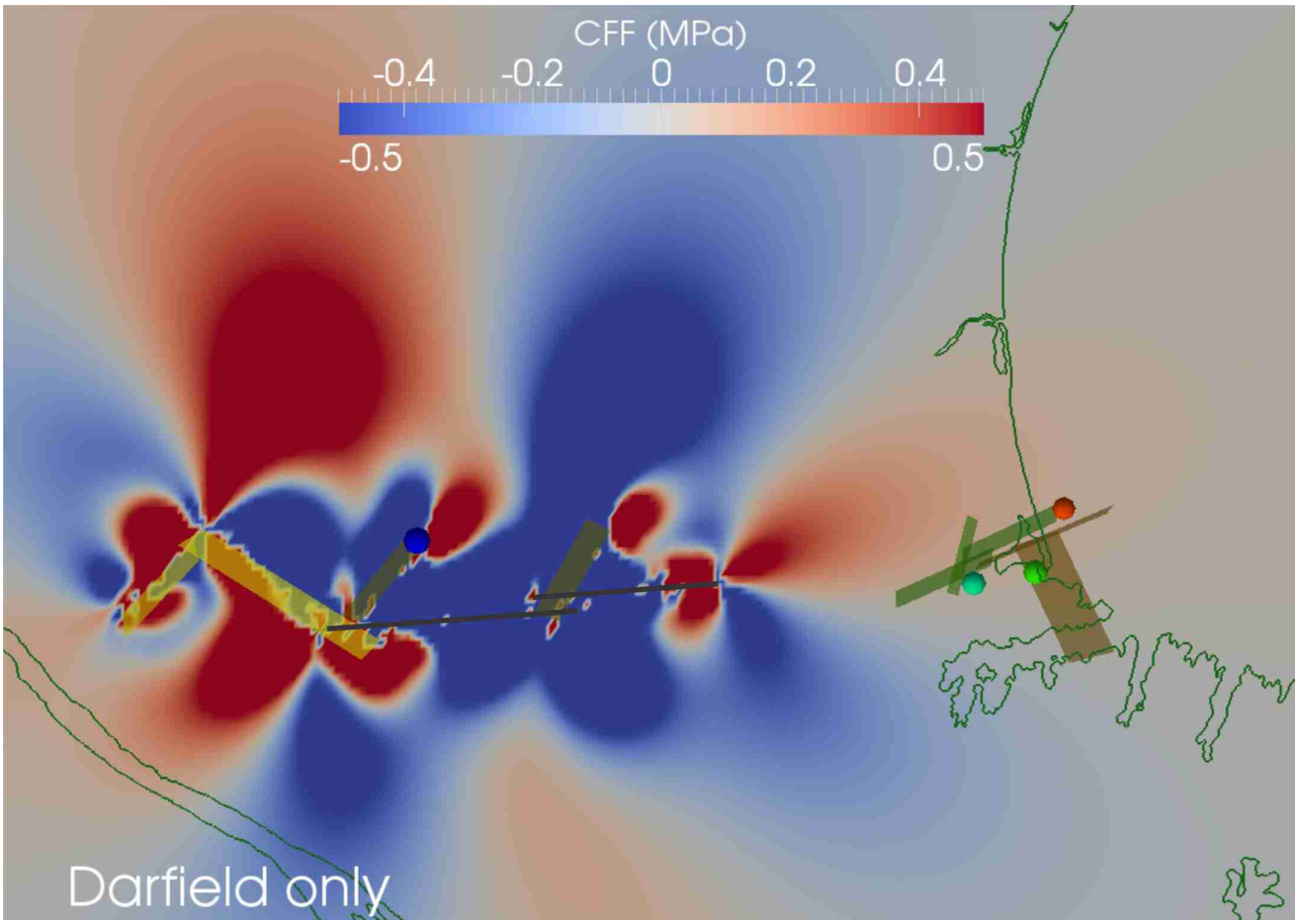

Figure 8.12: *Coulomb stress modelling for the Greendale Fault rupture (black line) after the Darfield earthquake and its effect on the Christchurch region resolved at a depth of 5 km. Green dots are the epicentres of the Christchurch earthquake and June 2011 earthquakes, and the red dot indicates the epicentral region of the Pegasus Bay earthquakes. Fault segments (green/brown/yellow rectangular regions) are those of Beavan et al. (2012). The eastern end where the Christchurch earthquake occurred is a small region where the failure stress increased due to the Darfield earthquake.*

bury earthquakes can be regarded as an intraplate sequence, remote from the main Alpine-Marlborough fault system that defines the Pacific/Australian plate boundary (e.g. Sibson *et al.* 2013; Fry *et al.* 2014). Considerable research is still required to fully characterise the complexity of the entire Canterbury earthquake sequence. However, preliminary modelling involving seismology, geodesy, finite-element source-modelling and geology has provided much data constraining interpretations for the earthquake sequence. Over a period of many months the Canterbury earthquake sequence evolved from a relatively standard aftershock sequence of the M_W 7.1 Darfield earthquake into a complex, long lasting series of earthquakes (Figure 8.13). By early 2014, the aftershock activity in the Canterbury region had decreased significantly compared with 2012; however, the probability for significant aftershocks, e.g. $M \geq 5$, remains high (Table 8.3). There are still many questions about why the Darfield earthquake and subsequent Canterbury aftershock sequence occurred where it did, and what effect it will have on the potential for future earthquakes in the region.

One feature of the aftershock sequence that has generated considerable debate is the region that has become known as "the gap" (e.g. Bannister and Gledhill 2012). The Greendale Fault rupture of the Darfield earthquake terminated $\backsim$15 – 20 km west of Christchurch, and the Christchurch earthquake

Table 8.2: *Expected and observed numbers of aftershocks later in the Canterbury sequence.*

Date (NZST)	Expected number of aftershocks M 4.0 - 4.9	Observed	Expected number of aftershocks $M >= 5.0$	Observed
22 - 28 February - M_W 6.2	12 - 29	67	0 - 5	3
1 - 7 March	1 - 10	4	0 - 2	1
8 - 14 March	0 - 6	7	0 - 2	0
15 - 21 March	2 - 11	1	0 - 2	0
22 - 28 March	0 - 7	2	0 - 2	0
29 March - 4 April	0 - 5	2	0 - 1	0
5 - 11 April	0 - 4	1	0 - 1	0
12 - 18 April	0 - 4	1	0 - 1	1
19 April - 18 May	2 - 11	7	0 - 2	2
19 May - 13 June	1 - 10	5	0 - 2	3
13 June - 12 July - M_W 6.0	11 - 28	46	0 - 5	3
13 July - 12 August	1 - 10	2	0 - 2	1
13 August - 12 September	1 - 8	9	0 - 2	0
13 September - 12 October	0 - 7	7	0 - 2	1

Table 8.3: *Aftershock probabilities for given magnitude ranges.*

Date	M 5.0 - 5.9			M 6.0 - 6.9			M 7.0+		
2 Mar 2011	34%	68%	98%	4%	10%	32%	0.40%	1%	3.5%
1 Nov 2013	n/a	11%	68%	n/a	1%	9%	n/a	0.07%	0.7%
1 Apr 2014	n/a	10%	70%	n/a	1%	9%	n/a	<1%	1%

was centred SE of the city centre. Between the eastern end of the Greendale Fault rupture zone and Christchurch city there is a region of decreased aftershock activity where no large ($M > 6.0$) aftershocks have occurred. The moment release in this region is less than that to the west or to the east despite continued aftershock activity (Beavan *et al.* 2012; Elliot *et al.* 2012). If this region were to rupture in a single event it could produce a M 6.0 – 6.5 earthquake. Bannister and Gledhill (2012) noted that focal mechanisms for the largest aftershocks suggest a degree of NNW-SSE left-lateral faulting, which would indicate short fault segments that may not be capable of generating larger earthquakes. However, right-lateral strike-slip faulting is likely towards the western edge of southern Christchurch. The likelihood of a large aftershock in the gap is nevertheless unresolved.

Another concern is the effect of the Canterbury earthquake sequence on faults outside the aftershock zone. Steacy *et al.* (2014) examined stress changes from all the main Canterbury events and found a stress increase of up to 0.24 MPa on the Porter's Pass Fault – an active fault ∽80 km NW of Christchurch capable of generating a M_W 7.5 earthquake. In the Canterbury Plains most of the aftershock activity has been located close to the Greendale Fault and the inferred fault segments. In the Christchurch region, the aftershock activity is more diffuse with most of it not closely associated with the various inferred fault segments. This may suggest increased fracturing of the crust beneath Christchurch, but the nature of the faulting remains unclear. The Canterbury region consists of strong, brittle crust, with no shallow brittle-ductile transition. The geology of the region is complicated by the presence of Banks Peninsula,

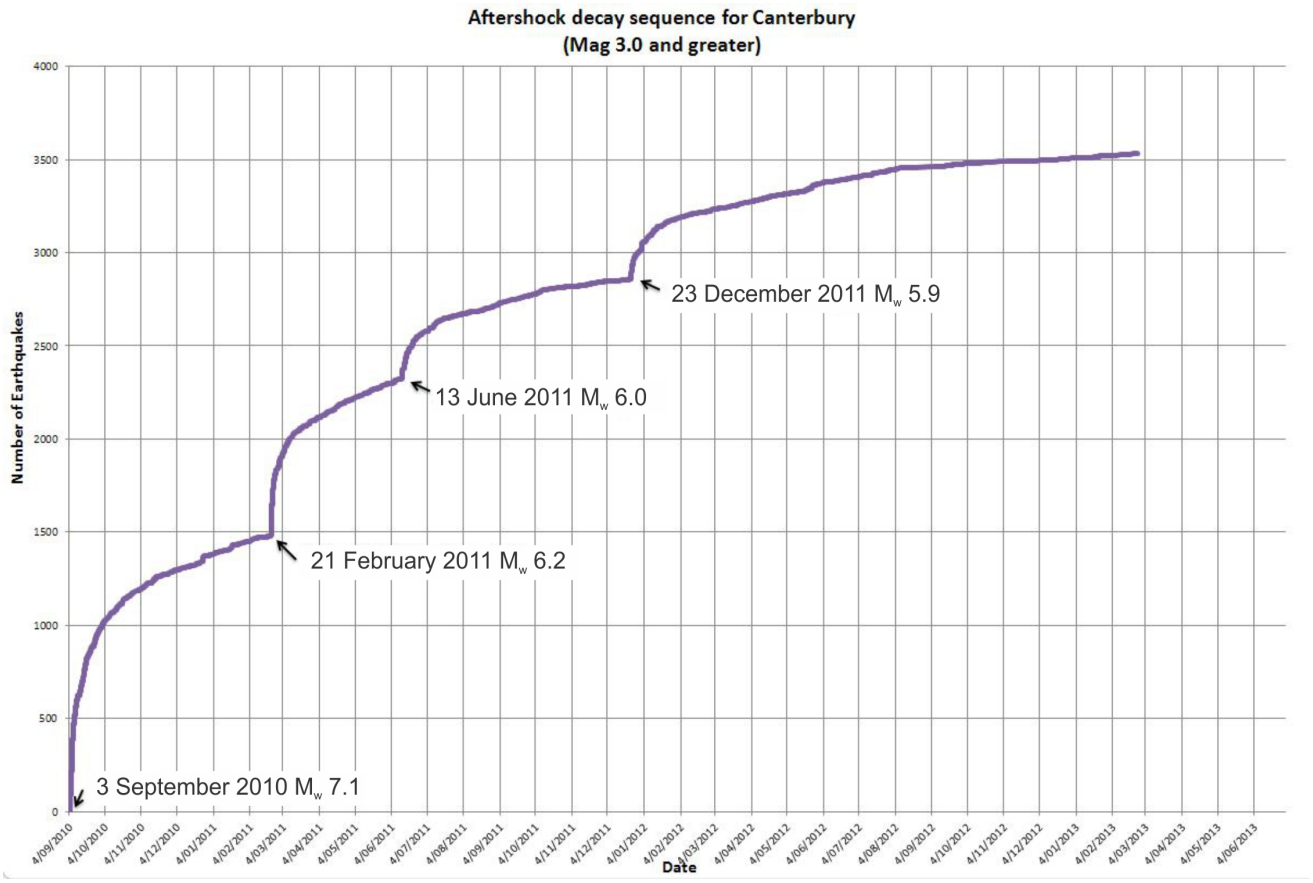

Figure 8.13: *Aftershock decay ($M \geq 3$) for the Canterbury earthquake sequence showing an increase in aftershock activity following each of the main earthquakes in the sequence.*

an intraplate, basaltic shield volcano that was active 12 – 6 Myr ago. What part this structure played in concentrating changes in Coulomb failure stress from the Darfield earthquake near Christchurch is a question that still needs addressing.

8.1.7 Conclusions

The M_W 6.2 February Christchurch earthquake was the deadliest and most damaging earthquake in New Zealand since the 3 February 1931 Hawkes Bay earthquake (M_W 7.4 – 7.6). As a result of the network of strong-motion instruments in operation in the Canterbury Plains and Christchurch regions before the Darfield and Christchurch mainshock occurrences, the Canterbury earthquake sequence is one of the best recorded earthquake sequences anywhere in the world. The near-field strong-motion dataset will be invaluable to future seismic hazard and engineering studies, in New Zealand and elsewhere in the world. The Canterbury earthquake sequence will influence thinking on seismic hazard and risk in New Zealand and worldwide for decades to come. We have learned a great deal about the Canterbury earthquake sequence since the initial 3 September 2010 M_W 7.1 Darfield earthquake; however, a great deal of research is still needed to fully understand the complexity of the Canterbury earthquake sequence.

8.1.8 Acknowledgements

This paper would not have been possible without many valuable discussions and much input from Stephen Bannister, John Beavan, Anne-Marie Christophersen, Susan Ellis, Bill Fry, Matt Gerstenberger, Caroline Holden, Anna Kaiser, Martin Reyners, Rick Sibson, Sandy Steacy and Charles Williams. Several of the figures were created using Generic Mapping Tools (GMT) (Wessel and Smith 1991). Figure 8.9 is from the author's collection: other photographic images are reproduced with kind permission of GNS Science/EQC.

8.1.9 References

Abercrombie, R.E., T.H. Webb, R. Robinson, P.G. McGinty, J. Mori, and R.J. Beavan (2000). The enigma of the Arthur's Pass, New Zealand earthquake 1. Reconciling a variety of data for an unusual earthquake sequence. *Journal of Geophysical Research* 105, 16119-16137.

Anderson, H., and T. Webb (1994). New Zealand seismicity: patterns revealed by the upgraded national seismograph network. *New Zealand Journal of Geology and Geophysics* 37, 477-493.

Atkinson, G.M., and D.M. Boore (2006). Earthquake ground-motion prediction equations for eastern North America. *Bulletin of the Seismological Society of America* 96, 2181-2205.

Aoi, S., T. Kunugi, and H. Fujiwara (2008). Trampoline effect in extreme ground motion. *Science* 322, 727-730, doi:10.1126/science.1163113

Atzori, S., C. Tolomei, A. Antonioli, J.P. Merryman Boncori, S. Bannister, E. Trasatti, P. Pasquali, and S. Salvi (2012). The 2010-2011 Canterbury, New Zealand, seismic sequence: multiple source analysis from InSAR data and modeling. *Journal of Geophysical Research* 117, B08305, doi:10.1029/2012JB009178

Avery, H.R., J.B. Berrill, P.F. Coursey, B.L. Deam, M.B. Dewe, C.C. Francois, J.R. Pettinga, and M.D. Yetton (2004). The Canterbury University strong-motion recording project. Proceedings of 13th World Conference on Earthquake Engineering, Vancouver, British Columbia, 1-6 August 2004. *Canadian Association for Earthquake Engineering* paper no. 1335.

Bannister, S., B. Fry, M. Reyners, J. Ristau, and H. Zhang (2011). Fine-scale relocation of aftershocks of the 22 February M_W 6.2 Christchurch earthquake using double-difference tomography. *Seismological Research Letters* 82, 839-845, doi:10.1785/gssrl.82.6.839

Bannister, S., and K. Gledhill (2012). Evolution of the 2010-2012 Canterbury earthquake sequence. *New Zealand Journal of Geology and Geophysics* 55, 295-304, doi:10.1080/00288306.2012.680475

Beavan, J., E. Fielding, M. Motagh, S. Samsonov, and N. Donnelly (2011). Fault location and slip distribution of the 22 February 2011 M_W 6.2 Christchurch, New Zealand earthquake from geodetic data. *Seismological Research Letters* 82, 789-799, doi:10.1785/gssrl.82.6.789

Beavan, J., M. Motagh, E. Fielding, N. Donnelly, and D. Collett (2012). Fault slip models of the 2010-2011 Canterbury, New Zealand, earthquakes from geodetic data, and observations of postseismic ground deformation. *New Zealand Journal of Geology and Geophysics* 55, 207-221, doi:10.1080/00288306.2012.697472

Berryman, K.R., U.A. Cochran, K.J. Clark, G.P. Biasi, R.M. Langridge, and P. Villamor (2012). Major earthquakes occur regularly on an isolated plate boundary. *Science* 336, 1690-1693, doi:10.1126/science.1218959

Bradley, B.A. (2013). Ground motions observed in the Darfield and Christchurch earthquakes and the importance of local site response effects. *New Zealand Journal of Geology and Geophysics* 55, 279-286, doi:10.1080/00288306.2012.674049

Bradley, B.A., and M. Cubrinovski (2011). Near-source strong ground motions observed in the 22 February 2011 Christchurch earthquake. *Seismological Research Letters* 82, 853-865, doi:10.1785/gssrl.82.6.853

Choy, G.L., J.L. Boatwright, and S. Kirby (2001). The radiated seismic energy and apparent stress of interplate and intraplate earthquakes at subduction zone environments: implications for seismic hazard estimate. *USGS Open-File Report* 01-005, 10 p.

Cochran, E.S., J.F. Lawrence, C. Christensen, and R.S. Jakka (2009). The Quake-Catcher Network: citizen science expanding seismic horizons. *Seismological Research Letters* 80, 26-30.

Cochran, E.S., J.F. Lawrence, A. Kaiser, B. Fry, A. Chung, and C. Christensen (2011). Comparison between low-cost and traditional MEMS accelerometers: a case study from the M 7.1 Darfield, New Zealand, aftershock deployment. *Annals of Geophysics* 54, 728-737, doi:10.4401/ag-5268

Cooper, A.F., and R.J. Norris (1990). Estimates for timing of the last coseismic displacement on the Alpine fault, northern Fiordland, New Zealand. *New Zealand Journal of Geology and Geophysics* 33, 309-307.

Cowan, H.A. (1991). The North Canterbury earthquake of September 1, 1888. *Bulletin of the New Zealand Society for Earthquake Engineering* 43, 222-227.

Cox, S.C., H.K. Rutter, A. Sims, M. Manga, J.J. Weir, T. Ezzy, P.A. White, T.W. Horton, and D. Scott (2012). Hydrological effects of the M_W 7.1 Darfield (Canterbury) earthquake, 4 September 2010, New Zealand. *New Zealand Journal of Geology and Geophysics* 55, 231-247, doi:10.1080/00288306.2012.680474

Cubrinovski, M., K. Robinson, M. Taylor, M. Hughes, and R. Orense (2012). Lateral spreading and its impacts in urban areas in the 2010-2011 Christchurch earthquakes. *New Zealand Journal of Geology and Geophysics* 55, 255-269, doi:10.1080/00288306.2012.699895

Dorn, C., A.G. Green, R. Jongens, S. Carpentier, A.E. Kaiser, F. Campbell, H. Horstmeyer, J. Campbell, M. Finnemore, and J. Pettinga (2010). High-resolution seismic images of potentially seismogenic structures beneath the northwest Canterbury Plains, New Zealand. *Journal of Geophysical Research* 115, B11303, doi:10.1029/2010JB007459

Doser, D.I., T.H. Webb, and D.E. Maunder (1999). Source parameters of large historical (1918-1962) earthquakes, South Island, New Zealand. *Geophysical Journal International* 139, 769-794.

Elliot, J.R., E.K. Nissen, P.C. England, J.A. Jackson, S. Lamb, Z. Li, M. Oehlers, and B. Parsons (2012). Slip in the 2010-2011 Canterbury earthquakes, New Zealand. *Journal of Geophysical Research* 117, B03401, doi:10.1029/2011jb008868

Fleischman, R.B., J.I. Restrepo, S. Pampanin, J.R. Maffei, K. Seeber, and F.A. Zahn (2014). Damage evaluations of precast concrete structures in the 2010-2011 New Zealand earthquake sequence. *Earthquake Spectra* 30, 277-306, doi:10.1193/031213EQS068M

Fry, B., and M.C. Gerstenberger (2011). Large apparent stresses from the Canterbury earthquakes of 2010 and 2011. *Seismological Research Letters* 82, 833-838, doi:10.1785/gssrl.82.6.833

Fry, B., R. Benites, and A. Kaiser (2011). The character of accelerations in the M_W 6.2 Christchurch earthquake. *Seismological Research Letters* 82, 846-852, doi:10.1785/gssrl.82.6.846

Fry, B., F.J. Davey, D. Eberhart-Phillips, and S. Lebedev (2014). Depth variable crustal anisotropy, patterns of crustal weakness, and destructive earthquakes in Canterbury, New Zealand. *Earth and Planetary Science Letters* 392, 50-57, doi:10.1016/j.epsl.2014.02.013

Gerstenberger, M., G. McVerry, D. Rhoades, and M. Stirling (2014). Seismic hazard modeling for the recovery of Christchurch, New Zealand. *Earthquake Spectra* 30, 17-29, doi:10.1193/021913EQS037M

Gledhill, K., R., Robinson, R. Abercrombie, T. Webb, J. Beavan, J. Cousins, and D. Eberhart-Phillips (2000). The M_W 6.2 Cass, New Zealand earthquake of 24 November 1995: reverse faulting in a strike-slip regime. *New Zealand Journal of Geology and Geophysics* 43, 255-269.

Holden, C. (2011). Kinematic source model of the 22 February 2011 M_W 6.2 Christchurch earthquake using strong-motion data. *Seismological Research Letters* 82, 783-788, doi:10.1785/gssrl.82.6.783

Holden, C., and J. Beavan (2012). Kinematic source studies of the ongoing (2010-2011) sequence of recent large earthquakes in Canterbury. Paper 061 (8 p) in Implementing lessons learnt: 2012 Conference, 13-15 April, Christchurch, New Zealand, Christchurch: *New Zealand Society for Earthquake Engineering.*

Kaiser, A., C. Holden, J. Beavan, D. Beetham, R. Benites, A. Celentano, D. Collet, J. Cousins, M. Cubrinovski, G. Dellow, P. Denys, E. Fielding, B. Fry, M. Gerstenberger, R. Langridge, C. Massey, M. Motagh, N. Pondard, G. McVerry, J. Ristau, M. Stirling, J. Thomas, S.R. Uma, and J. Zhao (2012). The M_W 6.2 Christchurch earthquake of February 2011: preliminary report. *New Zealand Journal of Geology and Geophysics* 55, 67-90, doi:10.1080/00288306.2011.641182

Lawrence, J.F., E.S. Cochran, A. Chung, A. Kaiser, C.M. Christensen, R. Allen, J.W. Baker, B. Fry, T. Heaton, D. Kilb, M.D. Kohler and M. Taufer (2014). Rapid earthquake characterization using MEMS accelerometers and volunteer hosts following the M 7.2 Darfield, New Zealand, earthquake. *Bulletin of the Seismological Society of America* 104, 184-192, doi:10.1785/0120120196

Massey, C.I., M.J. McSaveney, T. Taig, L. Richards, N.J. Litchfield, D.A. Rhoades, G.H. McVerry, B. Lukovic, D.W. Heron, W. Ries, and R.J. Van Dissen (2014). Determining rockfall risk in Christchurch using rockfalls triggered by the 2010-2011 Canterbury earthquake sequence. *Earthquake Spectra* 30, 155-181, doi:10.1193/021413EQS026M

Petersen, T., K. Gledhill, M. Chadwick, N.H. Gale, and J. Ristau (2011). The New Zealand national seismograph network. *Seismological Research Letters* 82, 9-20, doi:10.1785/gssrl.82.1.9

Reid, C.M., N.K. Thompson, J.R.M. Irvine, and T.E. Laird (2012). Sand volcanoes in the Avon-Heathcote estuary produced by the 2010-2011 Christchurch earthquakes: implications for geological preservation and expression. *New Zealand Journal of Geology and Geophysics* 55, 249-254,

doi:10.1080/00288306.2012.674051

Reyners, M., D. Eberhart-Phillips, and S. Martin (2014). Prolonged Canterbury earthquake sequence linked to widespread weakening of strong crust. *Nature Geoscience* 7, 34-37, doi:10.1038/ngeo2013

Rhoades, D.A., and R.J. Van Dissen (2003). Estimates of the time varying hazard of rupture of the Alpine fault, New Zealand, allowing for uncertainties. *New Zealand Journal of Geology and Geophysics* 46, 479-488.

Ristau, J. (2011). Focal mechanism analysis of Christchurch boxing day aftershocks. *GNS Science Consultancy Report* 2011/43, 7 p.

Ristau, J., C. Holden, A. Kaiser, C. Williams, S. Bannister, and B. Fry (2013). The Pegasus Bay aftershock sequence of the M_W 7.1 Darfield (Canterbury), New Zealand earthquake. *Geophysical Journal International* 195, 444-459, doi:10.1093/gji/ggt222

Serra, E.M.T., B. Delouis, A. Emolo, and A. Zollo (2013). Combining strong-motion, InSAR and GPS data to refine the fault geometry and source kinematics of the 2011, M_W 6.2 Christchurch earthquake (New Zealand). *Geophysical Journal International* 194, 1760-1777, doi:10.1093/gji/ggt186

Sibson, R., F. Ghisetti, and J. Ristau (2011). Stress control of an evolving strike-slip fault system during the 2010-2011 Canterbury, New Zealand, earthquake sequence. *Seismological Research Letters* 82, 824-832, doi:10.1785/gssrl.82.6.824

Sritharan, S., K. Beyer, R.S. Henry, Y.H. Chai, M. Kowalsky, and D. Bull (2014). Understanding poor seismic performance of concrete walls and design implications. *Earthquake Spectra* 30, 307-334, doi:10.1193/021713EQS036M

Steacy, S., A. Jiménez, and C. Holden (2014). Stress triggering and the Canterbury earthquake sequence. *Geophysical Journal International* 196, 473-480, doi:10.1093/gji/ggt380

Stirling, M., M. Gerstenberger, N. Litchfield, G. McVerry, W. Smith, J. Pettinga, and P. Barnes (2008). Seismic hazard of the Canterbury region, New Zealand: new earthquake source model and methodology. *Bulletin of the New Zealand Society for Earthquake Engineering* 41, 51-67.

Sutherland, R.D. *et al.* (2007). Do great earthquakes occur on the Alpine fault in central South Island, New Zealand?, in A Continental Plate Boundary: Tectonics at South Island, New Zealand, p. 235-251, eds. Okaya, D., Stern, T., and Davey, F., Geophysical Monograph 175, *American Geophysical Union*, Washington, DC.

Suzuki, W., S. Aoi, and H. Sekiguchi (2010). Rupture process of the 2008 Iwate-Miyagi Nairiku, Japan, earthquake derived from near-source strong-motion records. *Bulletin of the Seismological Society of America* 100, 256-266.

Wessel, P., and W.H.F. Smith (1991). Free software helps map and display data. *EOS Transactions* AGU 71, 441.

Yamada, M., J. Mori, and T. Heaton (2009). The slapdown phase in high-acceleration records of large earthquakes. *Seismological Research Letters* 80, 559-564, doi:10.1785/gssrl.80.4.559

Yetton, M.D., A. Wells, and N. Traylen (1998). The probability and consequences of the next Alpine

fault earthquake, *EQC Research Report* 95/193, New Zealand Earthquake Commission, Wellington, New Zealand.